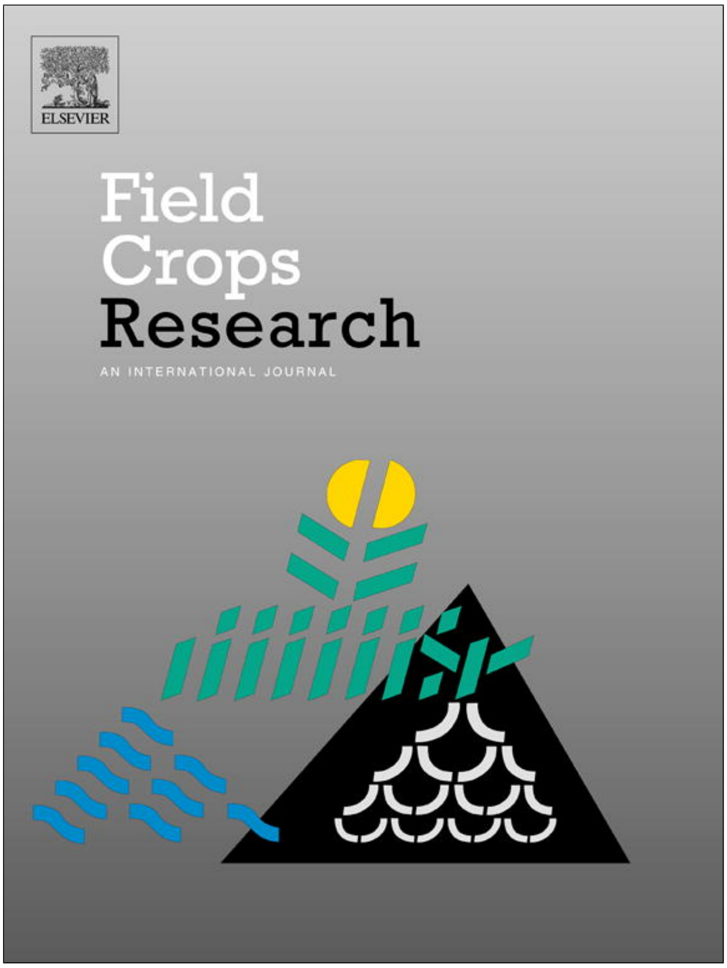
ELSEVIER
Field Crops Research
AN INTERNATIONAL JOURNAL

Field Crops Research 138 (2012) 21–32

Contents lists available at SciVerse ScienceDirect

Field Crops Research

journal homepage: www.elsevier.com/locate/fcr

Remotely estimating aerial N status of phenologically differing winter wheat cultivars grown in contrasting climatic and geographic zones in China and Germany

Fei Li[a,b], Bodo Mistele[b], Yuncai Hu[b], Xianlu Yue[b], Shanchao Yue[c], Yuxin Miao[c], Xinping Chen[c], Zhenling Cui[c], Qingfeng Meng[c], Urs Schmidhalter[b,*]

[a] College of Ecology & Environmental Science, Inner Mongolia Agricultural University, 010019, Hohhot, China
[b] Department of Plant Sciences, Technische Universität München, Emil-Ramann-Str. 2, D-85350, Freising-Weihenstephan, Germany
[c] College of Resources & Environmental Sciences, China Agricultural University, 100094, Beijing, China

ARTICLE INFO

Article history:
Received 22 December 2011
Received in revised form 3 September 2012
Accepted 3 September 2012

Keywords:
CCCI
Nitrogen fertilisation
NPDI
Red edge
Satellite
Vegetation indices

ABSTRACT

Red light based broadband vegetation indices are widely applied to derive aerial nitrogen (N) status parameters. With the advance of growth stages, however, crop canopy structure and aerial biomass will vary greatly, which negatively influences the relationships between spectral indices and the crop canopy N status. The current research aimed to assess the performance of red edge based vegetation indices, derived from simulated broadband WorldView-2 data, to remotely sense aerial N concentration and uptake in winter wheat (*Triticum aestivum* L.). Six experiments with different N rates for five German cultivars and four Chinese cultivars of winter wheat were conducted in southeast Germany and in the North China Plain from 2007 to 2010. The results showed that aerial biomass strongly affected the relationships between broadband vegetation indices and aerial N concentration before the heading stage. Normalising by using the planar domain index approach significantly improved the prediction power of red edge dependent broadband vegetation indices in estimating aerial N status. The two-dimensional broadband canopy chlorophyll content index (CCCI) and a newly proposed nitrogen planar domain index (NPDI) involving the WorldView-2 satellite red edge region were found to be more stable and better predictors than traditional red light based broadband vegetation indices in estimating aerial N concentration after the heading stage and in assessing aerial N uptake before the heading stage. The findings from this study may be useful for managing the application of N fertiliser for winter wheat in Zadoks growth stages 30–55 and in indirectly monitoring aerial N content in Zadoks growth stages 59–75 at landscape scales.

1. Introduction

Nitrogen (N) is one of the most active elements in agro-ecosystems (Smil, 2002) and the major element enhancing plant growth and influencing quality in nutrient resource management of crops (Ladha et al., 2005). Nitrogen sufficiency and N deficiency significantly affect the photosynthesis of crops, resulting in spectral variation of the canopy (Hatfield et al., 2008). Above ground plant N concentration and uptake, which are important indicators of the N status of winter wheat, are used to optimise nitrogen fertiliser applications (Mistele and Schmidhalter, 2008a, 2010). To match crop N requirements with soil N supply, an option in crop production is to use in-season measurements of the plant N status to fine-tune fertiliser N application (Scharf et al., 1993). However, crop N indicators are variable among fields and years as well as within a field (Scharf et al., 2005; Schmidhalter et al., 2006; Hong et al., 2007; Mistele and Schmidhalter, 2008b). Real-time and accurate detection of crop N concentration and uptake is important for optimising N management in crop production and avoiding environmental pollution (Stone et al., 1996; Schmidhalter et al., 2008).

Research shows that it is unfeasible to quickly quantify crop N variability both temporally and spatially at the regional scale using a point sampling estimation (Pinter et al., 2003). The development of satellite remote sensing has made it possible to estimate crop N status at field and regional scales. The most well-known and widely used approach for satellite-based remote sensing is the use of vegetation indices to derive the bio-physical and bio-chemical parameters of plants. However, the common red- and green-based broadband normalized difference vegetation index (NDVI) is strongly affected by factors, such as the soil background, canopy structure and chlorophyll distribution in the canopy (Daughtry et al., 2000; Haboudane et al., 2002) in early growth stages of crops but loses sensitivity for deriving agronomic parameters in later growth stages under moderate-to-high biomass conditions (Thenkabail

* Corresponding author. Tel.: +49 8161 713390; fax: +49 8161 714500.
E-mail address: schmidhalter@wzw.tum.de (U. Schmidhalter).

0378-4290/$ – see front matter © 2012 Elsevier B.V. All rights reserved.
http://dx.doi.org/10.1016/j.fcr.2012.09.002

et al., 2000; Flowers et al., 2003; Li et al., 2008; Erdle et al., 2011). To overcome these problems, a number of vegetation indices have been developed to estimate N-related indicators using remote sensing data for different types of crops. Rondeaux et al. (1996) developed the optimized soil adjusted vegetation index (OSAVI) by adding a parameter to minimise effects of soil on the crop canopy response. The NDVI was modified with a weighting coefficient ($WDRVI = (a \times R_{NIR} - R_{red})/(a \times R_{NIR} + R_{red})$) that increased the sensitivity of the NDVI to LAI (Gitelson, 2004). In addition, the commercially available high spatio-temporal resolution satellite data involving a red edge band may provide a new opportunity for monitoring and quantifying the N status at the canopy level (Eitel et al., 2007). Red edge, as the transition between the strong red light absorption by chlorophyll and the high near-infrared reflectance by plant tissue, is particularly sensitive to crop canopy chlorophyll and N variation compared with the other bands (Hatfield et al., 2008). Several studies have reported that broadband vegetation indices involving red edge information strongly improved the estimation power of agronomic parameters. Gitelson et al. (2005) used a conceptual model to develop the red edge chlorophyll index ($CI_{red\,edge} = R_{NIR}/R_{red\,edge} - 1$), which linearly relates to the canopy chlorophyll content in maize and soybean crops. To combine a physically based model with field validation, Eitel et al. (2008) proposed that the modified chlorophyll absorption ratio index (MCARI) combined with the second modified triangular vegetation index (MTVI2) (Haboudane et al., 2004) in a ratio of MCARI/MTVI2 improved spectral estimations of flag leaf N of dryland spring wheat. Based on the theory of two-dimensional planar domain illustrated by Clarke et al. (2001), the canopy chlorophyll content index (CCCI), including red, red edge and near-infrared bands, was presented as a method to extract N-related indicators for cotton (El-Shikha et al., 2008), wheat (Rodriguez et al., 2006; Tilling et al., 2007; Fitzgerald et al., 2006, 2010) and broccoli (El-Shikha et al., 2007). However, there has not yet been a detailed evaluation of the effects of growth stages and differences in the phenology of cultivars on the relationship between CCCI and N in contrasting regions.

To date, many vegetation indices have been derived to assess N-related agronomic indicators at both leaf and canopy levels for diverse vegetation species. Moreover, most of the high temporal and spatial resolution satellites, such as WorldView-2, which involves a single red edge band, have been launched in recent years. However, limited studies have been conducted to estimate winter wheat aerial N concentration and uptake at various growth stages using red edge based broadband vegetation indices with multi-temporal and multi-locational on-farm datasets. Thus, to improve nitrogen management and enhance crop productivity on a regional scale, there is a need to test and develop broadband vegetation indices for estimating in-season wheat aerial N concentration and uptake using newly launched satellite bands. The specific objectives of the present study were: (1) to enhance the stability and predictive power of broadband vegetation indices in estimating the aerial N concentration and uptake of winter wheat; (2) to validate and compare several known vegetation indices with red edge based indices in aerial N concentration and uptake prediction capability using ground truthing measurements collected from farmers' fields that were different from those used for calibration. The wheat cultivars used differed importantly in phenology and were grown under significantly contrasting conditions in China and Germany.

2. Materials and methods

2.1. Experimental sites

The experiments were conducted at two principal, contrasting locations, the Dürnast Experimental Station of the Technische Universität München (TUM) in Freising in Southeast Germany, and the Quzhou Experimental Station of the China Agricultural University (CAU) in Quzhou County located in the North China Plain. The average annual temperature in Freising is 7.5 °C and the yearly average precipitation is 800 mm with the highest values occurring in the winter wheat growing season (Mistele and Schmidhalter, 2010). Quzhou County lies in the warm-temperate subhumid-continental monsoon zone and is characterised by cold winters and hot summers. The yearly mean temperature is 13.1 °C, with 200 frost-free days. Annual average precipitation is 537 mm (average of 43 years from 1949 to 1992). However, the amount of precipitation during the wheat growing season is relatively small, i.e., 20% of total annual precipitation. Hence, farmers in this area irrigate winter wheat 3–4 times during the season by flood irrigation with water from wells, depending on the amount of precipitation during the growing season.

2.2. Experiment descriptions

2.2.1. Calibration experiments

The experiments, including three field experiments with incrementally increasing N levels (Experiments 1, 2 and 3), were used to establish the relationships between broadband vegetation indices and corresponding laboratory-measured aerial N concentration and uptake. Experiment 1 was performed at the Dürnast Research Station of the TUM in Freising, Germany, in 2008/2009. The soil was a Cambisol-type silty loam with a mineral N content of 56 kg ha^{-1}, CAL-P of 5 mg/100 g soil, CAL-K of 20 mg/100 g soil and pH value of 6.2 in the 0–30 cm layer. Three German winter wheat cultivars (Solitär, Ellvis and Tommi) and a Chinese cultivar (Nongda318) were planted on October 14, 2008. Nitrogen fertiliser applications with urea were split at three growth stages, i.e., GS 22, 32 and 47 (Zadoks et al., 1974), using eight rates (0, 60, 120, 180, 240, 300, 360 and 420 kg N ha^{-1}). The high rates were chosen to over-fertilisation as manifested in Chinese agriculture. The plot area was 4 m × 10 m with three replications. At the Quzhou experimental station of the CAU in 2009/2010, one German cultivar (Tommi) and two local cultivars (Heng4399 and Kenong9204) were used in experiment 2 with seven N rates (0, 60, 120, 180, 240, 300, 360 kg N ha^{-1}) based on residual soil mineral N previously assessed by a quick-test method (Schmidhalter, 2005). One Chinese wheat cultivar, Liangxing99, was used in experiment 3; the five N treatments were control (no N was applied), 50% of optimum N rate (Opt), 150% of Opt and conventional N rate (Con). The Opt was based on the aerial N requirement and the soil N supply for the two growing periods (sowing to shooting, shooting to harvest) (see Chen et al., 2006 for more details). The conventional N treatment represents the local farmers' practice, with 150 kg N ha^{-1} applied before sowing and 150 kg N ha^{-1} at the shooting stage as top-dressed fertiliser. All plots in experiments 2 and 3 received 54 kg P ha^{-1} as triple superphosphate and 75 kg K ha^{-1} as potassium sulphate before sowing. The soil in experiments 2 and 3 was a silt loam. The plot size was 4 m × 9 m with three replications in experiment 2 and 4 m × 10 m with four replications in experiment 3, respectively. The winter wheat Chinese cultivar Nongda318 was harvested on July 13, and the three German cultivars (Solitär, Ellvis and Tommi) were harvested on August 6, in 2009. In 2010, the two Chinese cultivars (Heng4399, Kenong9204) were harvested on June 18, and the German cultivar Tommi was harvested on July 7.

2.2.2. Validation experiments

Two farmers' fields grown with winter wheat at Gründerzentrum and Schafhof near the Dürnast Research Station of the TUM in 2007/2008 and five farmers' fields at Baizai Village near the Quzhou experimental station of the CAU in 2009/2010 were selected to validate the relationships between broadband vegetation indices and aerial N concentration and uptake. The experimental design in

Table 1
Spectral indices used in this study.

Vegetation index	Definition	Reference
Ratio vegetation index (RVI)	RVI = NIR/R	Jordan (1969)
Normalized difference vegetation index (NDVI)	NDVI = (NIR − R)/(NIR + R)	Rouse et al. (1974)
Normalized difference red edge index (NDRE)	NDRE = (NIR − RE)/(NIR + RE)	Barnes et al. (2000)
Optimized soil-adjusted vegetation index (OSAVI)	OSAVI = (1 + 0.16)(NIR − R)/(NIR + R + 0.16)	Rondeaux et al. (1996)
Wide dynamic range vegetation index (WDRVI)	WDRVI = (a × NIR − R)/(a × NIR + R) (a = 0.12)	Gitelson (2004)
Red edge chlorophyll index ($CI_{red\ edge}$)	$CI_{red\ edge}$ = NIR/RE − 1	Gitelson et al. (2005)
Second modified triangular vegetation index (MTVI2)	MTVI2 = 1.5[1.2(NIR − G) − 2.5(R − G)]/[(2NIR + 1)^2 − (6NIR − 5R$^{1/2}$) − 0.5]$^{1/2}$	Haboudane et al. (2004)
Modified chlorophyll absorption in reflectance index (MCARI)	MCARI = [(RE − R) − 0.2 × (RE − G)](RE/R)	Daughtry et al. (2000)
Transformed chlorophyll absorption in reflectance index (TCARI)	TCARI = 3 × [(RE − R) − 0.2 × (RE − G)(RE/R)]	Haboudane et al. (2002)
MCARI/OSAVI	MCARI/OSAVI	Daughtry et al. (2000)
TCARI/OSAVI	TCARI/OSAVI	Haboudane et al. (2002)
MCARI/MTVI2	MCARI/MTVI2	Eitel et al. (2007)
Canopy chlorophyll content index (CCCI)	CCCI = (NDRE − $NDRE_{MIN}$)/($NDRE_{MAX}$ − $NDRE_{MIN}$)	Barnes et al. (2000)
Nitrogen planar domain index (NPDI)	NPDI = ($CI_{red\ edge}$ − $CI_{red\ edge\ MIN}$)/($CI_{red\ edge\ MAX}$ − $CI_{red\ edge\ MIN}$)	This study

Gründerzentrum and Schafhof consisted of eight N rates (0, 60, 120, 180, 240, 300, 360 and 420 kg N ha^{-1}) with four replicates. The winter wheat cultivars used were Solitär, Pegasus, Ludwig and Cubus. six N rates (0, 60, 120, 180, 240, 300, 360 kg N ha^{-1}) were applied in selected farmers' fields in Baizai Village. The different farmers' fields were used as replications. Local cultivars were used, and the fields were managed by the farmers.

2.3. Spectral measurements

A passive spectrometer (tec5, Oberursel, Germany) was used in 2008, 2009 and 2010 (Mistele and Schmidhalter, 2010). In 2008, the device was mounted on a tractor to collect the reflectance information of winter wheat canopy (see Erdle et al., 2011 for more details). In 2009 and 2010, canopy spectral reflectance was measured using a Handy-Spec® field spectrometer. The measuring head of this device consists of two optics: the upper one is used to quantify the incoming light as reference, and the lower one records the reflectance from the vegetation and ground. The sensors can measure 256 bands with a spectral detection range from 300 to 1150 nm and have a bandwidth of 3.3 nm. Depending on the length of the plots, we measured reflectance in the winter wheat by holding the sensor approximately 0.8–1.0 m above the canopy and walking at the same speed in each plot. Before biomass sampling, the sensing was performed in all wheat plots, and the sensor path was parallel to the sowing rows.

Because we were considering using satellite image based broadband vegetation indices to detect crop N status at the regional scale in the future, we calculated the average of the reflectance measurements at the canopy scale according to WorldView-2 and RapidEye satellite bands: 510–580 and 520–590 nm as green (G), 630–690 and 630–685 nm as red (R), 705–745 and 690–730 nm as red edge (RE) and 770–895 and 760–850 nm as near infrared (NIR) bands, respectively. Nine single indices (RVI, NDVI, NDRE, OSAVI, WDRVI, $CI_{red\ edge}$, MTVI2, MCARI and TCARI) and five combined indices (MCARI/OSAVI, TCARI/OSAVI, MCARI/MTVI2, CCCI and NPDI) were then calculated and are presented in Table 1. Similar to the canopy chlorophyll content index (CCCI) (Fitzgerald et al., 2010), the N planar domain index (NPDI) is a two-dimensional index determined by the planar domain index approach reported by Clarke et al. (2001) (Fig. 1). The NPDI uses the NDVI to estimate the percentage of crop cover and the red edge chlorophyll index ($CI_{red\ edge}$), which is sensitive to the plant nitrogen status. The NPDI was calculated as follows

$$NDVI = \frac{NIR - R}{NIR + R}$$

$$CI_{red\ edge} = \frac{NIR}{RE} - 1$$

$$NDPI = \frac{\text{Measured } CI_{red\ edge} - CI_{red\ edge\text{-}}MIN}{CI_{red\ edge\text{-}}MAX - CI_{red\ edge\text{-}}MIN}$$

where $CI_{red\ edge}$-MIN is the value of $CI_{red\ edge}$ expected at a given crop cover (NDVI) for minimum canopy plant N or chlorophyll concentrations; and $CI_{red\ edge}$-MAX is the $CI_{red\ edge}$ value expected at a given crop cover for maximum plant N or chlorophyll concentrations.

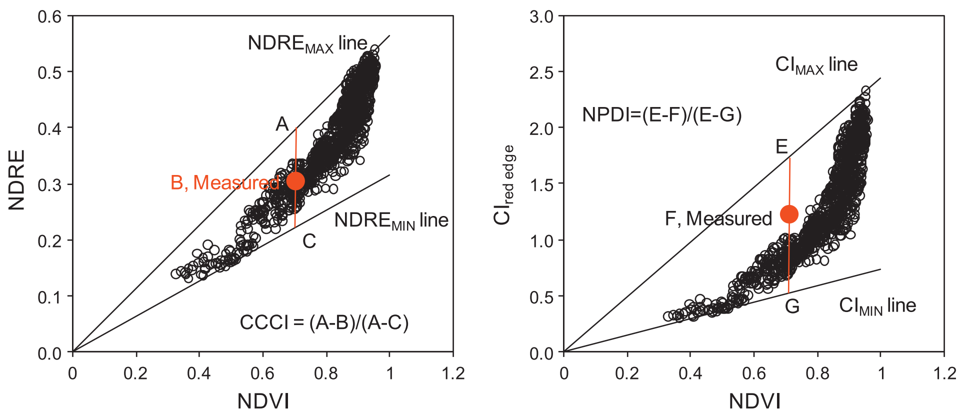

Fig. 1. Relationship between NDRE, $CI_{red\ edge}$ and NDVI used to derive the CCCIi and NPDIi from the NDVI, NDRE and $CI_{red\ edge}$.

2.4. Plant sampling and measurements

Above ground biomass was destructively sampled by randomly cutting five 1 m consecutive rows in each plot or farmer's field within the scanned areas immediately after reflectance measurements. All plant samples were oven dried at 70 °C to constant weight and then weighed and ground for chemical analysis later. A subsample was taken from the ground samples for Kjeldahl-N determination. The aerial N uptake was determined by multiplying aerial N concentration by dry biomass.

2.5. Statistical analysis

The correlations between plant N nutrient indicators and broadband vegetation indices were analysed using SAS software (SAS Institute, 1990). Data collected from validation experiments were used mainly for developing the regression models to establish the relationships of vegetation indices of the canopy with aerial N concentration and aerial N uptake, and data collected from validation experiments were used to validate the regression models under different cultivation conditions. The overall performance of the model was estimated by comparing the differences in the coefficient of determination (R^2), root mean square error (RMSE) and relative error (RE, %) of prediction. The higher the R^2 and the lower the RMSE and RE, the higher the precision and accuracy of the model will be for predicting aerial N uptake and concentration. Sensitivity of the different spectral vegetation indices to detect changes in aerial N concentration and uptake was tested through the use of the noise equivalent (NE) as the method reported by Viña and Gitelson (2005) and Viña et al. (2011).

$$\mathrm{NE} = \frac{\mathrm{RMSE}\left\{\text{VI vs. aerial N concentration or uptake}\right\}}{\mathrm{d}\,(\mathrm{VI})/\mathrm{d}\,(\text{aerial N concentration or uptake})}$$

where d(VI)/d(aerial N concentration or uptake) is the first derivative of the best-fit function of the relationship "spectral indices vs. aerial N concentration and uptake". The NE can conduct a comparison among different spectral indices in dynamic ranges.

3. Results

3.1. Variations in plant N and spectral data

As expected, different winter wheat cultivars, phenological stages and N fertiliser management strategies (from 0 to 420 kg N ha^{-1}), together with different sites and years, caused considerable variation in the above ground aerial N uptake and aerial N concentration. In each of the datasets taken from different growth stages, sites and years, aerial N uptake varied more than 42-fold and aerial N concentration varied more than 8-fold in the calibration experiments, while varying more than 11-fold for aerial N uptake and eight-fold for aerial N concentration in the validation experiments (Table 2). The high variation of aerial N uptake and concentration in the investigated fields resulted in datasets that were suitable for developing and validating regression models between broadband indices and plant N-related indicators. In addition, reflectance at G particular at RE are sensitive to aerial N uptake within a wide range of its variation compared with the R and NIR bands (Fig. 2).

3.2. Relationships between vegetation indices and aerial N concentration and uptake

The German winter wheat cultivars are awnless, taller and ripened later compared with the Chinese cultivars. To understand the effects of growth stages and cultivars on the relationships between spectral indices and aerial N concentration and uptake, we performed regression correlations controlling for vegetative (before heading) and reproductive (after heading) growth periods and for the growth environments in Southeast Germany and the North China Plain. According to the values of the R^2 in Table 3, the broadband vegetation indices calculated from simulated WorldView-2 satellite bands having the strongest correlations with aerial N uptake were NPDIi (R^2 = 0.76), CCCIi (R^2 = 0.75) and then $CI_{red\,edge}$ (R^2 = 0.68) and NDRE (R^2 = 0.61), regardless of cultivars. However, better correlations between indices and aerial N uptake were observed only for German cultivars at the reproductive growth period, indicating that a difference in canopy structure of cultivars after heading affected the relationships between the indices and aerial N uptake. For aerial N concentration, vegetation indices generally were better correlated at the reproductive growth period than those at the vegetative growth period. Similarly, vegetation indices NPDIi, CCCIi, $CI_{red\,edge}$ and NDRE were more closely related to aerial N concentration compared with the other indices at the reproductive growth period.

Regression results from the different sites at different years showed that the R^2 values for relationship between the vegetation indices NPDIi, CCCIi, $CI_{red\,edge}$ and NDRE and aerial N uptake were generally higher than those for the relationship between vegetation indices and aerial N concentration (Table 3). In comparison, regression results for the single indices OSAVI, TCARI, MCARI and MTVI2 and combined indices TVARI/OSAVI, MCARI/OSAVI and MCARI/MTVI2 showed poor relationships ($R^2 \sim 0$), which may result from broadband information confounding the spectral resolution or from the broad range of cultivars, growth conditions and growing seasons.

Across all growth stages, cultivars, sites and years, red edge based vegetation indices $CI_{red\,edge}$ (R^2 = 0.59), NDRE (R^2 = 0.54), CCCIi (R^2 = 0.71) and the newly proposed index NPDIi (R^2 = 0.67) were more strongly correlated with aerial N uptake than the other vegetation indices (Table 3). Overall, red edge based indices generally were more correlated with plant N status indicators than red light based vegetation indices because red edge, to a degree, was more sensitive than other parts of the bands when quantifying plant N status.

Table 2
Descriptive statistics of aerial N concentration and N uptake for calibration and validation experiments in vegetative (GS 30–55) and reproductive (GS 59–75) growth periods.

	n	Aerial N uptake (kg N ha^{-1})				Aerial N concentration (%)			
		Range	Mean	SD	CV(%)	Range	Mean	SD	CV(%)
Calibration experiments									
Vegetative growth period	389	9–292	82	58	70.3	1.1–5.6	3.4	0.88	25.8
Reproductive growth period	234	37–386	170	71	42.0	0.7–3.4	1.9	0.53	27.5
All	623	9–386	118	76	66.4	0.7–5.6	2.8	1.04	36.3
Validation experiments									
Vegetative growth period	183	30–248	118	50	42.8	1.4–4.8	3.0	0.81	26.6
Reproductive growth period	115	44–328	182	78	43.1	0.6–2.1	1.3	0.42	32.4
All	298	30–328	143	70	49.1	0.6–4.8	2.4	1.08	45.9

3.3. Model establishment

Nitrogen nutrient management at the vegetative growth period plays an important role during the wheat growth period because wheat plants take up the most N before heading. Thus, real-time detection of aerial N uptake before heading will be useful for developing N fertiliser management strategies for winter wheat. However, monitoring aerial N concentration after heading is important for guiding agricultural practice (Eitel et al., 2008) and decreasing the risk of environmental pollution.

On the basis of the R^2, relationships established between vegetation indices and the aerial N concentration and uptake (Table 3), we plotted the four best performing indices – NPDIi, CCCIi, $CI_{red\ edge}$ and NDRE calculated by using WorldView-2 and RapidEye satellite data – together with the aerial N uptake at the vegetative growth period and with the aerial N concentration at the reproductive growth period. As illustrated in Fig. 3, all four spectral indices were quadratic related to aerial nitrogen uptake regardless of the cultivar and phenological properties. Compared with NDRE and $CI_{red\ edge}$, the R^2 for CCCIi and NPDIi increased by 9.5–22.4% and 5.4–5.7%, respectively. The results indicate that normalising using the planar domain theory, as illustrated by Clarke et al. (2001), greatly improved the prediction of aerial N uptake. However, plots of broadband indices NDRE, $CI_{red\ edge}$, CCCIi and NPDIi against aerial N concentration (Fig. 4) did not show an obviously improved response of CCCIi and NPDIi over that of NDRE and $CI_{red\ edge}$.

3.4. Evaluation and validation of the model

Except R^2 as a statistical characteristic for the established model, it is important to assess sensitivity of each performing well spectral index to aerial N concentration and uptake. In order to evaluate how sensitive of VIs to aerial N concentration and uptake, we used the method of the noise equivalent (NE) as mentioned by Viña and Gitelson (2005) and Viña et al. (2011) to compare the NE of NDRE, $CI_{red\ edge}$, CCCIi and NPDIi. As illustrated in Fig. 5, The NE of NPDIi in aerial N uptake was the lowest among the four VIs tested. For NE in aerial N concentration, NDRE and CCCIi had much higher noise equivalent when aerial N concentration exceeded 2%.

To test the robustness of predicting N status by using selected broadband spectral indices, an established model for detecting crop N uptake and concentration should be applied over wide phenological and cultural conditions. Thus, the evaluation was based on a comparison of the aerial N uptake and N concentration predicted by the best performing indices, with aerial N uptake and concentration measured analytically for independent datasets involving different German and Chinese wheat cultivars from farmers' fields of southeastern Germany and the North China Plain.

The validation results according to the statistical analysis for the best performing indices, $CI_{red\ edge}$, NDRE, CCCIi and the newly proposed index NPDIi, are shown in Figs. 6 and 7. For N uptake varying from 30 to 248 kg N ha^{-1} at the vegetative growth period (Table 2), the RMSE and RE of aerial N uptake prediction using simulated WorldView-2 satellite data did not exceed 35 kg N ha^{-1} and 30%, respectively, which is acceptable under heterogeneous

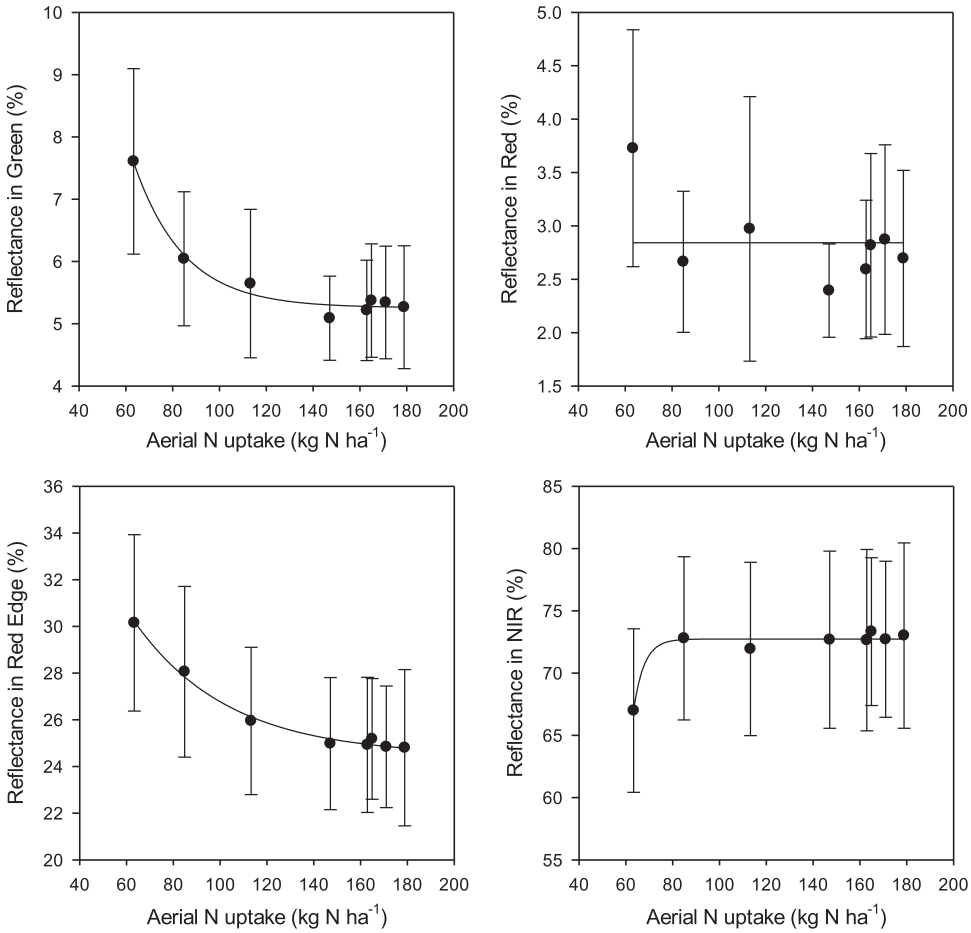

Fig. 2. Relationship between aerial N uptake and wheat canopy reflectance in R (630–690 nm), G (510–580 nm), RE (705–745 nm) and NIR (770–895 nm) bands across cultivars, sites and years.

Table 3
Coefficient of determination (R^2) for relationships between spectral indices (calculated from WorldView-2 satellite bands) and aerial N concentration and uptake across cultivars, growth stages, sites and years.

Spectral indices	Vegetative growth period (GS 30–55)			Reproductive growth period (GS 59–75)			Freising, Germany (2008/2009)			Quzhou, China (2009/2010)			All
	German cultivar	Chinese cultivar	Combined	German cultivar	Chinese cultivar	Combined	German cultivar	Chinese cultivar	Combined	German cultivar	Chinese cultivar	Combined	
Aerial N concentration													
RVI	0.06	0.24**	0.02	0.66**	0.29**	0.52**	0.02	0.24**	0.08*	0.28**	0.31**	0.20**	0.00
NDVI	0.13**	0.18**	0.06**	0.63**	0.40**	0.37**	0.00	0.39**	0.07*	0.40**	0.21**	0.24****	0.04
NDRE	0.10**	0.22**	0.03	0.67**	0.41**	0.46**	0.03	0.13**	0.00	0.32**	0.27**	0.25**	0.06
WDRVI	0.11**	0.24**	0.06**	0.67**	0.37**	0.44**	0.00	0.34**	0.07*	0.38**	0.29**	0.26**	0.03
$CI_{red\ edge}$	0.09*	0.25**	0.03	0.70**	0.37**	0.49**	0.02	0.10*	0.00	0.30**	0.30**	0.25**	0.06
OSAVI	0.01	0.04	0.01	0.64**	0.12*	0.23**	0.15**	0.62**	0.27**	0.17**	0.02	0.02	0.02
TCARI	0.00	0.05	0.00	0.47**	0.08	0.38**	0.07*	0.26**	0.12**	0.30**	0.29**	0.18**	0.01
MCARI	0.00	0.07	0.00	0.48**	0.15*	0.36**	0.19**	0.58**	0.28**	0.17**	0.01	0.02	0.04
MTVI2	0.01	0.02	0.00	0.62**	0.13*	0.24**	0.13**	0.68**	0.27**	0.13**	0.02	0.01	0.01
MCARI/OSAVI	0.00	0.06	0.00	0.42**	0.15*	0.34**	0.19**	0.57**	0.29**	0.18**	0.01	0.01	0.05
TCARI/OSAVI	0.01	0.04	0.01	0.49**	0.14*	0.39**	0.07*	0.33**	0.13**	0.36**	0.26**	0.21**	0.01
MCARI/MTVI2	0.00	0.06	0.00	0.34**	0.20**	0.33**	0.19**	0.53**	0.27**	0.27**	0.11*	0.06	0.05
CCCIi	0.04	0.18**	0.00	0.45**	0.32**	0.39**	0.07*	0.02	0.02	0.13**	0.21**	0.16**	0.09**
NPDIi	0.07	0.24**	0.02	0.61**	0.35**	0.47**	0.04	0.01	0.00	0.23**	0.28**	0.22**	0.07*
Aerial N uptake													
RVI	0.41**	0.45**	0.46**	0.27**	0.01	0.24**	0.18**	0.00	0.14**	0.83**	0.70**	0.75**	0.33**
NDVI	0.29**	0.44**	0.32**	0.31**	0.00	0.12*	0.22**	0.03	0.09**	0.54**	0.66**	0.53**	0.25**
NDRE	0.63**	0.63**	0.61**	0.65**	0.02	0.29**	0.67**	0.11**	0.50**	0.75**	0.76**	0.67**	0.54**
WDRVI	0.37**	0.47**	0.40**	0.30**	0.00	0.17**	0.21**	0.01	0.12**	0.68**	0.72**	0.64**	0.30**
$CI_{red\ edge}$	0.70**	0.64**	0.68**	0.68**	0.02	0.33**	0.70**	0.13**	0.55**	0.81**	0.77**	0.71**	0.59**
OSAVI	0.09*	0.00	0.15**	0.39**	0.13*	0.37**	0.04*	0.20**	0.00	0.30**	0.01	0.17**	0.12**
TCARI	0.01	0.02	0.04	0.09*	0.00	0.12**	0.00	0.07*	0.00	0.73**	0.58**	0.67**	0.04
MCARI	0.01	0.00	0.02	0.14**	0.08	0.33**	0.05*	0.43**	0.05	0.40**	0.07	0.26**	0.02
MTVI2	0.12**	0.00	0.18**	0.45**	0.15*	0.42**	0.06*	0.25**	0.01	0.29**	0.02	0.18**	0.15**
MCARI/OSAVI	0.00	0.01	0.04	0.09*	0.06	0.28**	0.07*	0.47**	0.08*	0.40**	0.07	0.25**	0.01
TCARI/OSAVI	0.03	0.02	0.09**	0.10*	0.00	0.11**	0.00	0.08*	0.00	0.72**	0.65**	0.68**	0.06
MCARI/MTVI2	0.00	0.00	0.02	0.04	0.00	0.15**	0.11**	0.49**	0.12**	0.49**	0.16*	0.35**	0.01
CCCIi	0.82**	0.64**	0.75**	0.70**	0.13*	0.42**	0.81**	0.70**	0.79**	0.81**	0.67**	0.63**	0.71**
NPDIi	0.78**	0.66**	0.76**	0.72**	0.03	0.39**	0.78**	0.37**	0.69**	0.85**	0.74**	0.71**	0.67**

* Significant at the 0.05 probability level.
** Significant at the 0.01 probability level.

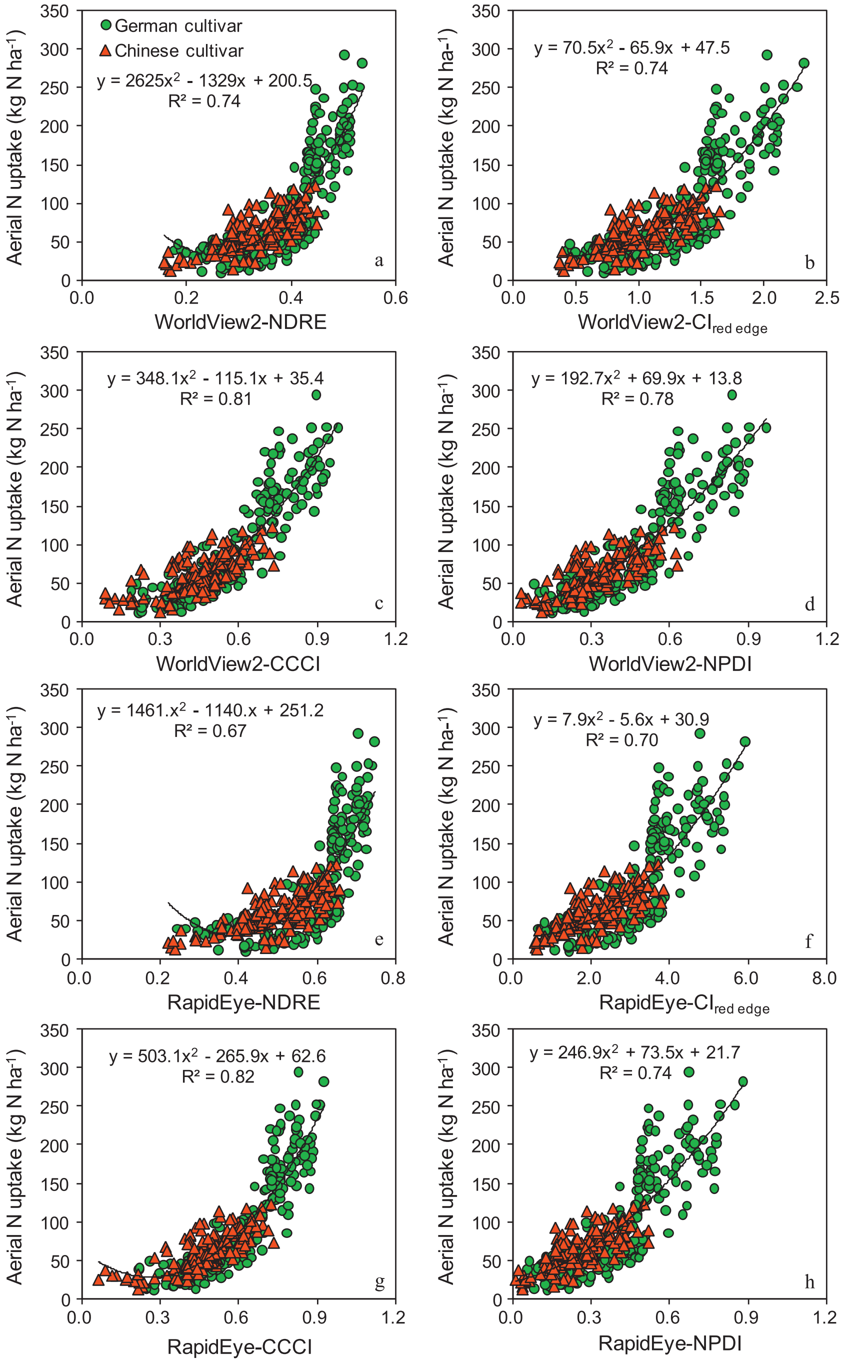

Fig. 3. Relationships between WorldView2-NDRE (a), WorldView2-$CI_{red\ edge}$ (b), WorldView2-CCCI (c) and WorldView2-NPDI (d), RapidEye-NDRE (e), RapidEye-$CI_{red\ edge}$ (f), RapidEye-CCCI (g), RapidEye-NPDI (h) and aerial N uptake before heading stage across cultivars, sites and years.

field conditions. The R^2 between estimated aerial N uptake and observed aerial N uptake was generally greater than 0.60. In comparison, the predicted N uptake by $CI_{red\ edge}$ and NDRE deviated much more from the 1:1 line (underestimation of N uptake) at higher N uptake, while for the aerial N concentration at the reproductive growth period, the validation performance for NPDIi and CCCIi was no better than $CI_{red\ edge}$ and NDRE (Fig. 7).

4. Discussion

The present study shows that the newly proposed two-dimensional NPDIi was strongly related to the ground-measured N status parameters, independent of the growing season, growth stage, study area and phenological properties. Of particular importance is that the relationships obtained between NPDIi and ground data were geographically transferable between completely different climate conditions (Figs. 8 and 9), i.e., fairly cool and wet in southeastern Germany and hot and dry in the North China Plain during the winter wheat growing period. Furthermore, the relationship developed was validated using independent datasets with local German cultivars (awnless and taller) and Chinese cultivars (awny and smaller) representing a wide range of cultivars grown on complex and heterogeneous farmers' fields in both southeastern Germany and the North China Plain. As shown in previous studies (El-Shikha et al., 2007, 2008; Rodriguez et al., 2006; Tilling et al., 2007; Fitzgerald et al., 2006, 2010), red edge indices developed

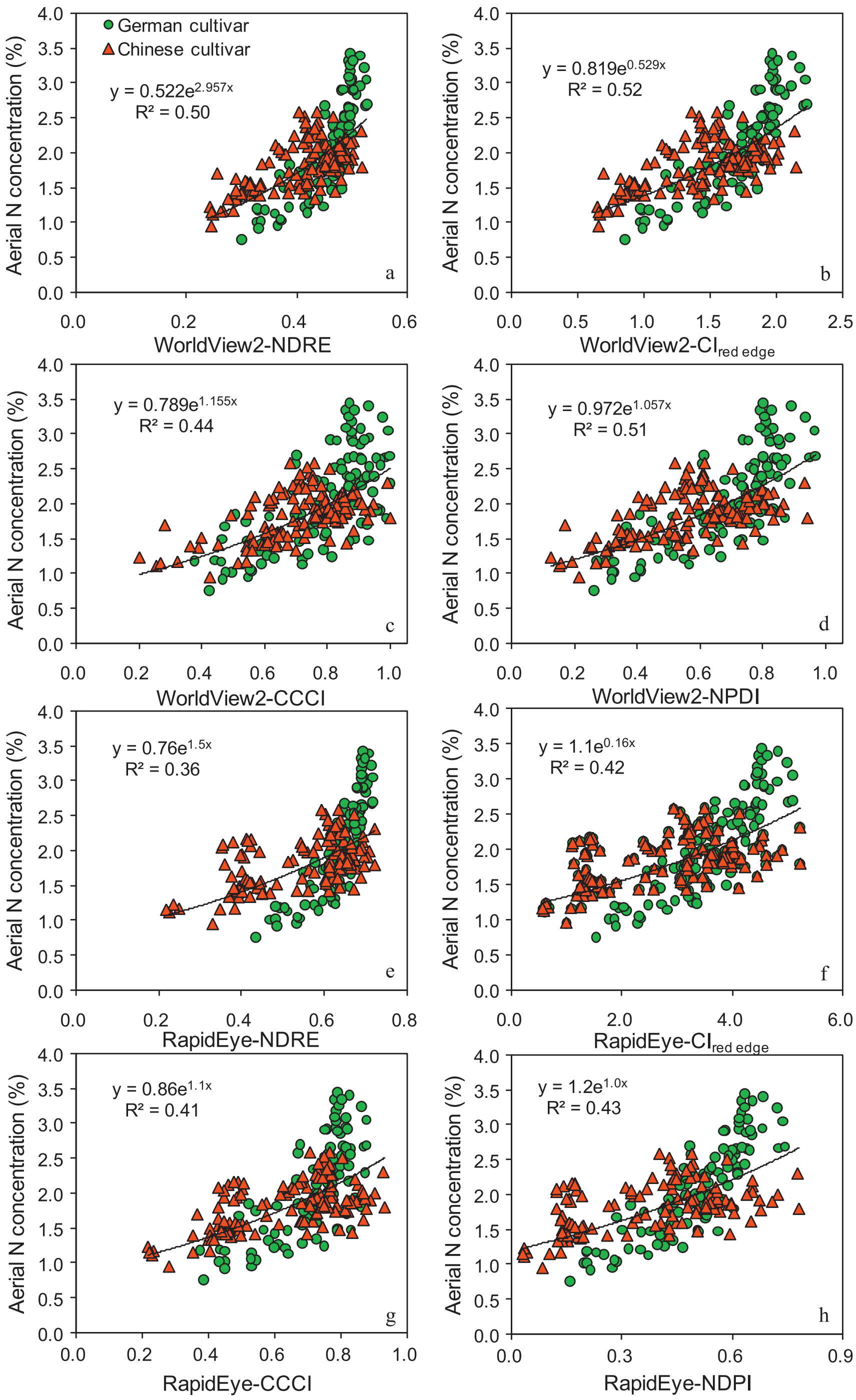

Fig. 4. Relationships between worldview2-NDRE (a), WorldView2-CI$_{red\ edge}$ (b), WorldView2-CCCI (c) and WorldView2-NPDI (d), RapidEye-NDRE (e), RapidEye-CI$_{red\ edge}$ (f), RapidEye-CCCI (g), RapidEye-NPDI (h) and aerial N concentration after heading stage across cultivars, sites and years.

with a two-dimensional approach (Clarke et al., 2001) were more sensitive and robust in deriving plant N-status-related parameters compared with red light based single and combined indices. A difference in the present study is that the two-dimensional indices were structured by using the broadband simulated WorldView-2 and RapidEye satellite data rather than narrow or short bands. The findings of Eitel et al. (2007, 2008) indicated that indices by broadband data reduced the predicting power of N status indicators because of a decreased spectral resolution. The results in this study show that normalisation by NDVI improved the response of two-dimensional broadband indices CCCIi and NPDIi over single and combined indices, suggesting that the planar domain theory mentioned by Barnes et al. (2000) and Clarke et al. (2001) increased the potential of using red edge based broadband satellite data.

The main goal of using multispectral satellite data to derive aerial N status indicators is to increase the sensitivity to N-related indicators of plants, while reducing the variation due to the crop canopy structure, aerial biomass and soil background reflectance. Thus, it is most important to select suitable vegetation index formulas and band combinations. In this study, selected broadband indices were poorly or not at all related to the aerial N concentration at Zadoks growth stages 30–55 combining all site-years or at the whole growing period in the same site-years (Table 3), which is in agreement with findings by Flowers et al. (2003) and Li et al.

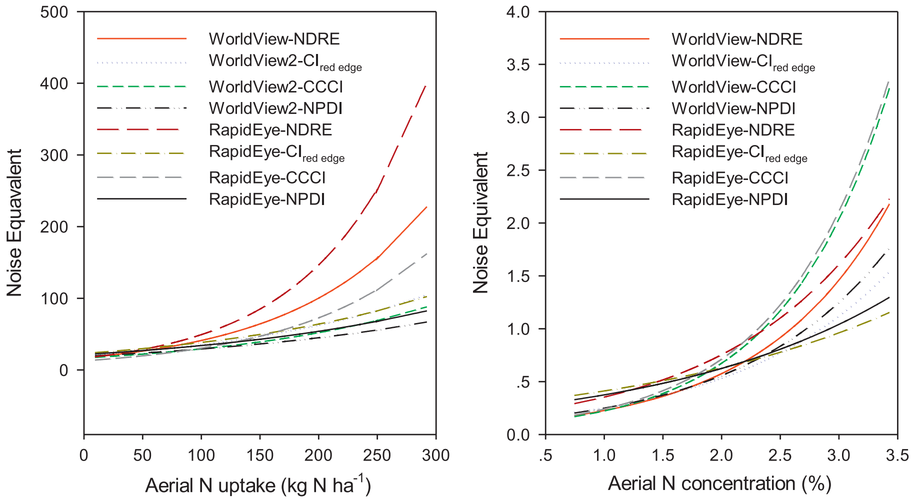

Fig. 5. Noise equivalent of aerial N concentration and uptake estimation by the broadband spectral indices of WorldView2-NDRE, WorldView2-CI$_{red\ edge}$, WorldView2-CCCI, WorldView2-NPDI, RapidEye-NDRE, RapidEye-CI$_{red\ edge}$, RapidEye-CCCI and RapidEye-NPDI.

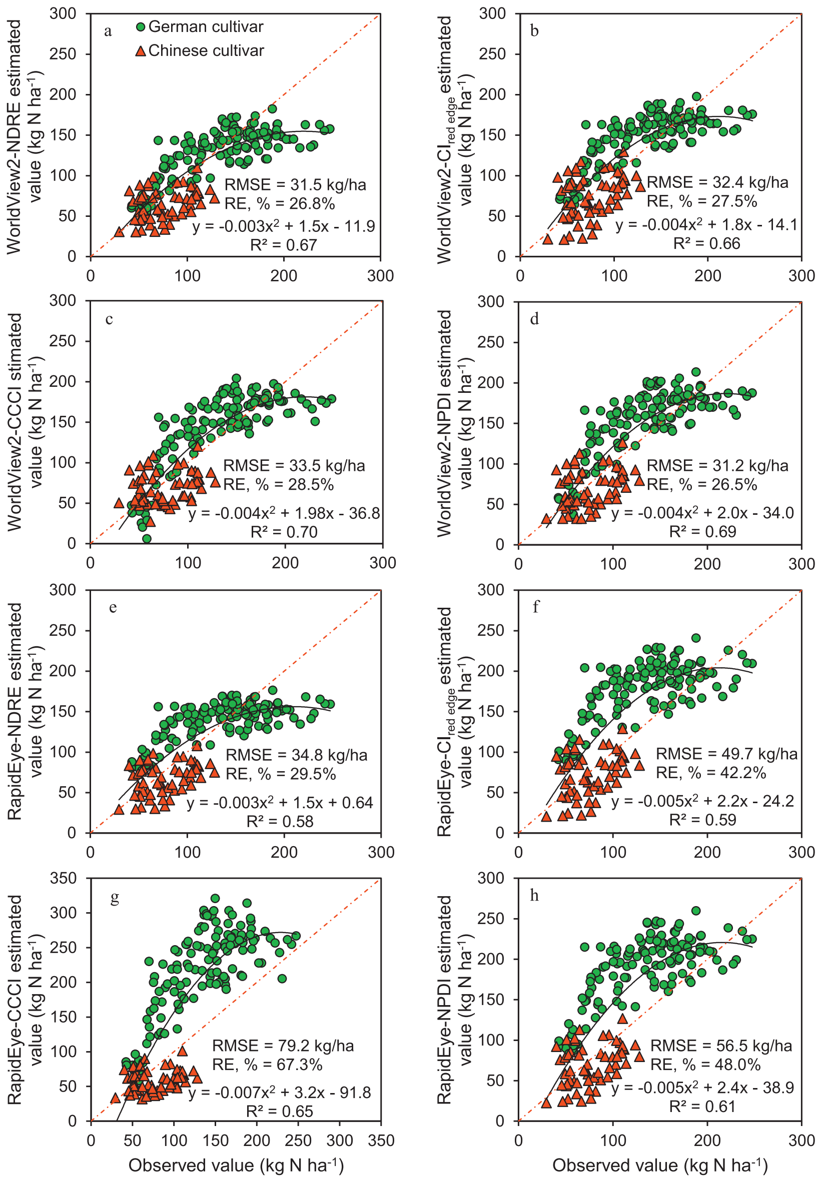

Fig. 6. Relationship between estimated and observed aerial N uptake for the data from farmers' fields before heading stage (a, b, c, d, e, f, g and h stand for WorldView2-NDRE, WorldView2-CI$_{red\ edge}$, WorldView2-CCCI, WorldView2-NPDI, RapidEye-NDRE, RapidEye-CI$_{red\ edge}$, RapidEye-CCCI and RapidEye-NPDI estimated value, respectively).

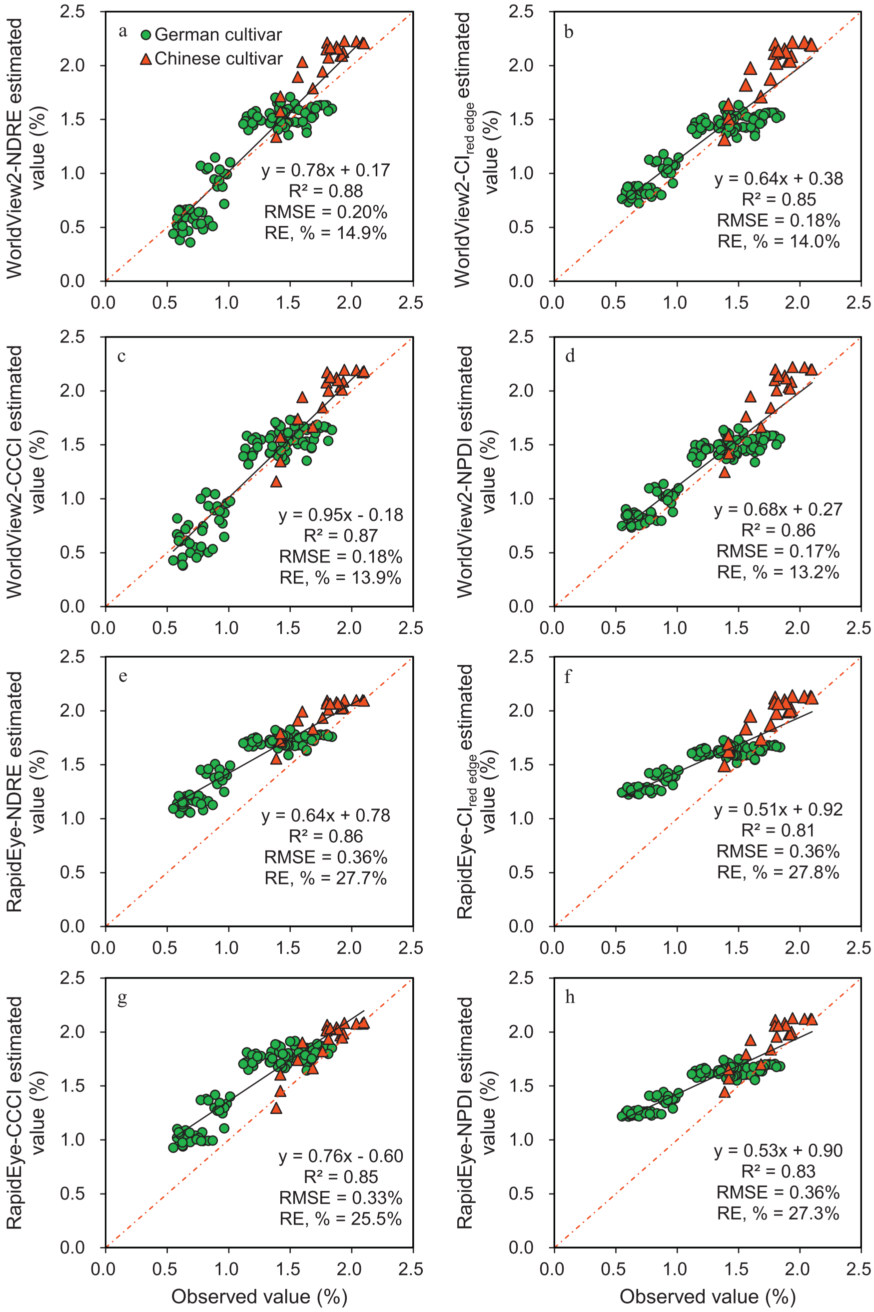

Fig. 7. Relationship between estimated and observed aerial N concentration for the data from farmer's fields after heading stage (a, b, c, d, e, f, g and h stand for WorldView2-NDRE, WorldView2-$CI_{red\ edge}$, WorldView2-CCCI, WorldView2-NPDI, RapidEye-NDRE, RapidEye- $CI_{red\ edge}$, RapidEye-CCCI and RapidEye-NPDI estimated value, respectively).

(2008). The findings indicate that variation of the leaf area index (LAI) and above ground biomass at different growth stages negatively affects the relationship between the indices and aerial N concentration. Before heading in particular, the growth stage has an important effect on the relationship between vegetation indices and aerial N concentration because aerial N uptake cannot keep pace with the aerial biomass increment (Table 3). Because crop canopy reflectance is a function of plant N and biomass, it is difficult to identify the plant N signature remotely using the biomass information. Furthermore, the aerial biomass of crops rapidly increased during the vegetative growth period, and the effects of the signature of aerial biomass on spectral reflectance were stronger compared with that of plant N before heading. The "dilution effect" of N may result in some inconsistency in extracting aerial N concentration using spectra-based information at periods when biomass is increasing rapidly (Flowers et al., 2003; Eitel et al., 2007). Thus, it is best to derive aerial N concentration using spectral vegetation indices at clearly defined growth stages before heading. Even though optimising narrow band vegetation indices to estimate the aerial N concentration was used to cover different growth stages before heading, the relationship between the selected vegetation indices and the aerial N concentration was negative and nonlinear, and the relationship was not robust compared with the aerial N uptake (Hansen and Schjoerring, 2003; Stroppiana et al., 2009)

As in the current study, Eitel et al. (2007, 2008) reported a significant correlation between aerial N concentration and the combined index MCARI/MTVI2 computed either by handheld CropScan multispectra data or by simulated RapidEye^{TM} satellite data at Zadoks growth stages 57–60 in three dryland spring wheat fields. However, they did not indicate whether the correlation was strong

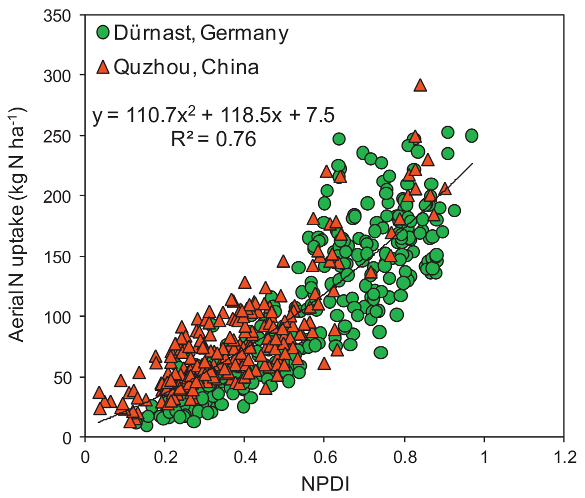

Fig. 8. Relationships between NPDI (calculated from simulated WorldView-2 satellite bands) and aerial N uptake covering all datasets at Dürnast (southeast Germany) and Quzhou (North China Plain) experimental stations.

before the heading stage. Our research shows that a significant relationship exists between selected indices and the whole aerial N concentration after the heading stage combining all site-years. An explanation for the relationship is that maximum above ground biomass was obtained at the heading stage, when the effect of dilution (Justes et al., 1994) diminishes. Thus, aerial N concentration has a more important effect on reflectance patterns than biomass does. The results reported by Bausch et al. (2008) for maize and Cohen et al. (2010) for potato further confirm the stronger relationships between satellite based broadband indices and leaf N concentration under dense canopies at late growth stages when the aerial biomass reaches constant values. In addition, better relationships were observed for the red edge based indices than for the red based indices.

In the current study, traditional single indices (i.e., NDVI, OSAVI, WDRVI, MTVI2, MCARI and TCARI) and combined indices (i.e., MCARI/OSAVI, TVARI/OSAVI and MCARI/MTVI2) using green or red light reflectance showed a poor relationship with aerial N uptake for all dataset formations (Table 3). The explanation for this is probably that NDVI-like broadband vegetation indices obtained by

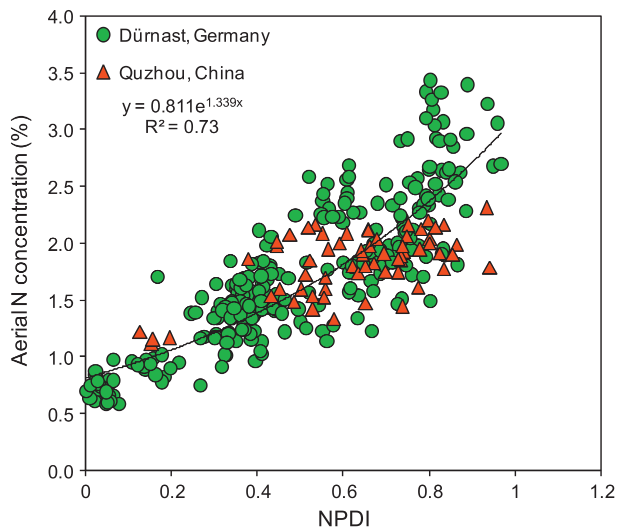

Fig. 9. Relationships between NPDI (calculated from simulated WorldView-2 satellite bands) and aerial N concentration covering all datasets at Dürnast (southeast Germany) and Quzhou (North China Plain) experimental stations.

traditional multispectral satellite bands are mostly based on the red light region, which loses sensitivity in predicting agronomic variables at moderate to high canopy cover or aerial biomass (Viña et al., 2004; Gitelson et al., 2003, 2005, 2006; Haboudane et al., 2008; Herrmann et al., 2011), thus limiting the usefulness of these broadband vegetation indices under high aerial N uptake (Flowers et al., 2003; Li et al., 2010). In contrast, Hively et al. (2009) reported that broadband NDVI derived from multispectral satellite SPOT 5 images effectively predicted aerial N uptake for rye, barley and wheat, but these results were based on a prediction of low aerial N uptake values at early growth stages. Similar to the findings of Li et al. (2008), broadband RVI based on simulated Quickbird satellite data was strongly related to aerial N uptake. In this study, however, the better performing broadband spectral indices were red edge based single indices NDRE, $CI_{red\ edge}$ and two-dimensional combined indices CCCIi and NPDIi. These findings suggest that the red edge region was the important spectral region in deriving aerial N status parameters when selecting a suitable spectral indices formula. A limitation is that the broadband CCCIi and NPDIi were tested only by using WorldView-2 and RapidEye satellites data. The red edge bands selection in different satellite data may affect the performance of indices in deriving aerial N status of wheat. In future, identifying optimal red edge band and its range for aerial N estimation need further to be conducted using bands optimum algorithm (Peng and Gitelson, 2011, 2012). Thus, depending specific satellite data, we can better use of new red edge based proposed spectral indices and performs further investigation with other crops. With the launch of high temporal-spatial resolution satellites involving the red edge region, the long-standing reliance on red light based broadband NDVI-like spectral indices is reduced.

In conclusion, our findings confirm that the two-dimensional broadband combined index CCCIi and, particularly, the newly proposed broadband index NPDIi were relatively stable and powerful indices for deriving aerial N uptake before the heading stage and aerial N concentration after the heading stage across sites, years, cultivars and phenological properties. Our results also provide useful insight for using satellite remote sensing to guide producers in managing their N application in the critical growth stages, such as at GS 30–36, for an enhanced N fertilizer use efficiency and to reduce the pollution potential by monitoring N concentrations after the heading stage. Further validation and testing will be needed to estimate the stability and transferability of the best performing spectral indices at heterogeneous wheat production agro-ecosystems using real satellite data involving red edge in the future.

Acknowledgement

This research was financially supported by the German Federal Ministry of Education and Research (BMBF) (Project No. FKZ 0330800A)

References

Barnes, E.M., Clarke, T.R., Richards, S.E., Colaizzi, P.D., Haberland, J., Kostrzewski, M., Waller, P., Choi, C., Riley, E., Thompson, T., Lascano, R.J., Li, H., Moran, M.S., 2000. Coincident detection of crop water stress, nitrogen status and canopy density using ground based multispectral data. In: Robert, P.C., Rust, R.H., Larson, W.E. (Eds.), Proc. 5th Int. Conf. Precis Agric. Bloomington, MN, USA.

Bausch, W.C., Halvorson, A.D., Cipra, J., 2008. Quickbird satellite and ground-based multispectral data correlations with agronomic parameters of irrigated maize grown in small plots. Biosys. Eng. 101, 306–315.

Chen, X.P., Zhang, F.S., Römheld, V., Horlacher, D., Schulz, R., Böning-Zilkens, M., Wang, P., Claupein, W., 2006. Synchronizing N supply from soil and fertilizer and N demand of winter wheat by an improved N_{min} method. Nutr. Cycl. Agroecosys. 74, 91–98.

Clarke, T.R., Moran, M.S., Barnes, E.M., Pinter Jr., P.J., Qi, J., 2001. Planar domain indices: a method for measuring a quality of a single component in two-component pixels. In: Proc. IEEE International Geosci. Remote Sens. Sympos, Sydney, Australia, 9–13 July.

Cohen, Y., Alchanatis, V., Zusman, Y., Dar, Z., Bonfil, D.J., Karnieli, A., Zilberman, A., Moulin, A., Ostrovsky, V., Levi, A., Brikman, R., Shenker, M., 2010. Leaf nitrogen estimation in potato based on spectral data and on simulated bands of the VENuS satellite. Precis. Agric. 11, 520–537.

Daughtry, C.S.T., Walthall, C.L., Kim, M.S., Colstoun, E.B., McMurtrey III, J.E., 2000. Estimating corn leaf chlorophyll concentration from leaf and canopy reflectance. Remote Sens. Environ. 74, 229–239.

Eitel, J.U.H., Long, D.S., Gessler, P.E., Smith, A.M.S., 2007. Using in situ measurements to evaluate the new RapidEye satellite series for prediction of wheat nitrogen status. Int. J. Remote Sens. 28, 4183–4190.

Eitel, J.U.H., Long, D.S., Gessler, P.E., Hunt, E.R., 2008. Combined spectral index to improve ground-based estimates of nitrogen status in dryland wheat. Agron. J. 100, 1694–1702.

El-Shikha, D.M., Waller, P., Hunsaker, D., Clarke, T., Barnes, E., 2007. Ground-based remote sensing for assessing water and nitrogen status of broccoli. Agric. Water Manage. 92, 183–193.

El-Shikha, D.M., Barnes, E.M., Clarke, T.R., Hunsaker, D.J., Haberland, J.A., Pinter Jr., P.J., Waller, P.M., Thompson, T.L., 2008. Remote sensing of cotton nitrogen status using the canopy chlorophyll content index (CCCIi). Trans. Am. Soc. Agric. Biol. Eng. 51, 73–82.

Erdle, K., Mistele, B., Schmidhalter, U., 2011. Comparison of active and passive spectral sensors in discriminating biomass parameters and nitrogen status in wheat cultivars. Field Crops Res. 124, 74–84.

Fitzgerald, G.J., Rodriguez, D., Christensen, L.K., Belford, R., Sadras, V., Clarke, T., 2006. Spectral and thermal sensing for nitrogen and water status in two wheat agroecosystems. Precis. Agric. 7, 233–248.

Fitzgerald, G.J., Rodriguez, D., O'Leary, G., 2010. Measuring and predicting canopy nitrogen nutrition in wheat using a spectral index—the canopy chlorophyll content index (CCCIi). Field Crops Res. 116, 318–324.

Flowers, M., Weisz, R., Heiniger, R., 2003. Quantitative approaches for using color infrared photography for assessing in-season nitrogen status in winter wheat. Agron. J. 95, 1189–1200.

Gitelson, A.A., Gritz, U., Merzlyak, M.N., 2003. Relationships between leaf chlorophyll content and spectral reflectance and algorithms for non-destructive chlorophyll assessment in higher plant leaves. J. Plant. Physiol. 160, 271–282.

Gitelson, A.A., 2004. Wide dynamic range vegetation index for remote quantification of biophysical characteristics of vegetation. J. Plant Physiol. 161, 165–173.

Gitelson, A.A., Viña, A., Ciganda, V., Rundquist, D.C., Arkebauer, T.J., 2005. Remote estimation of canopy chlorophyll content in crops. Geophys. Res. Lett. 32, L08403, http://dx.doi.org/10.1029/2005GL022688.

Gitelson, A.A., Keydan, G.P., Merzlyak, M.N., 2006. Three-band model for noninvasive estimation of chlorophyll, carotenoids, and anthocyanin contents in higher plant leaves. Geophys. Res. Lett., http://dx.doi.org/10.1029/2006GL026457.

Haboudane, D., Miller, J.R., Tremblay, N., Zarco-Tejada, P.J., Dextraze, L., 2002. Integrated narrowband vegetation indices for prediction of crop chlorophyll content for application to precision agriculture. Remote Sens. Environ. 81, 416–426.

Haboudane, D., Miller, J.R., Pattey, E., Zarco-Tejada, P.J., Strachan, I.B., 2004. Hyperspectral vegetation indices and novel algorithms for predicting green LAI of crop canopies: modeling and validation in the context of precision agriculture. Remote Sens. Environ. 90, 337–352.

Haboudane, D., Tremblay, N., Miller, J.R., Vigneault, P., 2008. Remote estimation of crop chlorophyll content using spectral indices derived from hyperspectral data. IEEE Trans. Geosci. Remote Sens. 46, 423–437.

Hansen, P.M., Schjoerring, J.K., 2003. Reflectance measurement of canopy biomass and nitrogen status in wheat crops using normalized difference vegetation indices and partial least square regression. Remote Sens. Environ. 86, 542–553.

Hatfield, J.L., Gitelson, A.A., Schepers, J.S., Walthall, C.L., 2008. Application of spectral remote sensing for agronomic decisions. Agron. J. 100, 117–131.

Herrmann, I., Pimstein, A., Karnieli, A., Cohen, Y., Alchanatis, V., Bonfil, D.J., 2011. LAI assessment of wheat and potato crops by VENμS and Sentinel-2 bands. Remote Sens. Environ. 115, 2141–2151.

Hively, W.D., Lang, M., McCarty, G.W., Keppler, J., Sadeghi, A., McConnell, L.L., 2009. Using satellite remote sensing to estimate winter cover crop nutrient uptake efficiency. J. Soil Water Conserv. 64, 303–313.

Hong, N., Scharf, P.C., Davis, G., Kitchen, N.R., Suddus, K.A., 2007. Economically optimal nitrogen rate reduces soil residual nitrate. J. Environ. Qual. 36, 354–362.

Jordan, C.F., 1969. Derivation of leaf area index from quality of light on the forest floor. Ecology 50, 663–666.

Justes, E., Mary, B., Meynard, J.M., Machet, J.M., Thelier-Huche, L., 1994. Determination of a critical nitrogen concentration dilution curve for winter wheat crops. Ann. Bot. 74, 397–407.

Ladha, J.K., Pathak, H., Krupnik, T.J., Six, J., van Kessel, C., 2005. Efficiency of fertilizer nitrogen in cereal production: retrospects and prospects. Adv. Agron. 87, 85–156.

Li, F., Gnyp, M.L., Jia, L., Miao, Y., Yu, Z., Koppe, W., Bareth, G., Chen, X., Zhang, F., 2008. Estimating N status of winter wheat using a handheld spectrometer in the North China Plain. Field Crops Res. 106, 77–85.

Li, F., Miao, Y.X., Chen, X.P., Zhang, H.L., Jia, L.L., Bareth, G., 2010. Estimating winter wheat biomass and nitrogen status using an active crop sensor. Intel. Autom. Soft Comput. 16, 1221–1230.

Mistele, B., Schmidhalter, U., 2008a. Estimating the nitrogen nutrition index using spectral canopy reflectance measurements. Eur. J. Agron. 29, 184–190.

Mistele, B., Schmidhalter, U., 2008b. Spectral measurements of the total aerial N and biomass dry weight in maize using a quadrilateral-view optic. Field Crops Res. 106, 94–103.

Mistele, B., Schmidhalter, U., 2010. Tractor-based quadrilateral spectral reflectance measurements to detect biomass and total aerial nitrogen in winter wheat. Agron. J. 102, 499–506.

Peng, Y., Gitelson, A.A., 2011. Application of chlorophyll-related vegetation indices for remote estimation of maize productivity. Agric. Forest Meteorol. 151, 1267–1276.

Peng, Y., Gitelson, A.A., 2012. Remote estimation of gross primary productivity in soybean and maize based on total crop chlorophyll content. Remote Sens. Environ. 117, 440–448.

Pinter, P.J., Hatfield, J.L., Schepers, J.S., Barnes, E.M., Moran, M.S., Daughtry, C.S.T., Upchurch, D.R., 2003. Remote sensing for crop management. Photogramm. Eng. Remote Sens. 69, 647–664.

Rondeaux, G., Steven, M., Baret, F., 1996. Optimization of soil-adjusted vegetation indices. Remote Sens. Environ. 55, 95–107.

Rodriguez, D., Fitzgerald, G.J., Belford, R., Christensen, L., 2006. Detection of nitrogen deficiency in wheat from spectral reflectance indices and basic crop ecobiophysiological concepts. Aust. J. Agric. Res. 57, 781–789.

Rouse, J.W., Haas, R.H., Schell, J.A., Deering, D.W., Harlan, J.C., 1974. Monitoring the vernal advancements and retrogradation of natural vegetation. Final rep. NASA/GSFC, Greenbelt, MD.

Scharf, P.C., Alley, M.M., Lei, Y.Z., 1993. Spring nitrogen on winter wheat: I. Farmer-field validation of tissue test-based rate recommendations. Agron. J. 85, 1181–1186.

Scharf, P.C., Kitchen, N.R., Sudduth, K.A., Glenn Davis, J., Hubbard, V.C., Lory, J.A., 2005. Field-scale variability in optimal nitrogen fertilizer rate for corn. Agron. J. 97, 452–461.

Schmidhalter, U., 2005. Development of a quick on-farm test to determine nitrate levels in soil. J. Plant Nutr. Soil Sci. 168, 432–438.

Schmidhalter, U., Bredemeier, C., Geesing, D., Mistele, B., Selige, T., Jungert, S., 2006. Precision agriculture: spatial and temporal variability of soil water, nitrogen and plant crop response. Bibliotheca Fragmenta Agronomica 11, 97–106.

Schmidhalter, U., Maidl, F.-X., Heuwinkel, H., Demmel, M., Auernhammer, H., Noack, P., Rothmund, M., 2008. Precision farming—adaptation of land use management to small scale heterogeneity. In: Schröder, P., Pfadenhauer, J., Munch, J.C. (Eds.), Perspectives for Agroecosystem Management. Elsevier, Amsterdam, The Netherlands, pp. 121–199.

Smil, V., 2002. Nitrogen and food production: Proteins for human diets. Ambio 31, 126–131.

Stone, M.L., Solie, J.B., Raun, W.R., Whitney, R.W., Taylor, S.L., Ringer, J.D., 1996. Use of spectral radiance for correcting in-season fertilizer nitrogen deficiencies in winter wheat. Trans. ASAE 39, 1623–1631.

Stroppiana, D., Boschetti, M., Brivio, P.A., Bocchi, S., 2009. Plant nitrogen concentration in paddy rice from field canopy hyperspectral radiometry. Field Crops Res. 111, 119–129.

Thenkabail, P.S., Smith, R.B., Pauw, E.D., 2000. Hyperspectral vegetation indices and their relationships with agricultural crop characteristics. Remote Sens. Environ. 71, 158–182.

Tilling, A.K., O'Leary, G.J., Ferwerda, J.G., Jones, S.D., Fitzgerald, G., Rodriguez, D., Belford, R., 2007. Remote sensing of nitrogen and water stress in wheat. Field Crops Res. 104, 77–85.

Viña, A., Henebry, G.M., Gitelson, A.A., 2004. Satellite monitoring of vegetation dynamics: sensitivity enhancement by the wide dynamic range vegetation index. Geophys. Res. Lett., http://dx.doi.org/10.1029/2003GL019034.

Viña, A., Gitelson, A.A., 2005. New developments in the remote estimation of the fraction of absorbed photosynthetically active radiation in crops. Geophy. Res. Lett. 32, L17403, http://dx.doi.org/10.1029/2005GL023647.

Viña, A., Gitelson, A.A., Nguy-Robertson, A.L., Peng, Y., 2011. Comparison of different vegetation indices for the remote assessment of green leaf area index of crops. Remote Sens. Environ. 115, 3468–3478.

Zadoks, J.C., Chang, T.T., Konzak, C.F., 1974. A decimal code for the growth stages of cereals. Weed Res. 14, 415–421.